Characterization of relaxed photo-excited magnetized states in prussian-blue analogous magnets

Toshihiko Yokoyama,[a] Kaoru Okamoto,[a] Daiju Matsumura,[a] Toshiaki Ohta[a] Shin-ichi Ohkoshi[b] and Kazuhito Hashimoto[b]

[a]Department of Chemistry, Graduate School of Science, The University of Tokyo, 7-3-1 Hongo, Bunkyo-ku, Tokyo 113-0033, Japan, [b]Research Center for Advanced Science and Technology, The University of Tokyo, 4-6-1 Komaba, Meguro-ku, Tokyo 153-0041, Japan.
E-mail: toshi@chem.s.u-tokyo.ac.jp

Local structure of a photo- or x-ray-induced ferrimagnet $Cs_{0.8}Co_{1.3}[W(CN)_8](3\text{-cyanopyridine})_{1.9}\cdot 2.1H_2O$ was investigated by means of Co *K*- and W *L*-edge XAFS spectroscopy. The Co *K*-edge XANES spectra provide quantitative information on the ratio of Co(II) and Co(III) by virtue of the factor analysis. It was found that the Co(II) ratios are 81.9% at 300 K and 32.7% at 150 K. When the sample was irradiated by x rays at 30 K, a phase transformation occurred in a similar manner to the visible-light irradiation and a relaxed excited state that exhibits ferrimagnetism was formed. The relaxed excited state gives the Co(II) ratio of 67.0%. The W L_{III}-edge EXAFS spectra determine the W-C, W-N and W-Co distances. The results of the distances were obtained as *R*(W-C)=2.16 Å, *R*(W-N)=3.31 Å, *R*(W-Co^{II})=5.37 Å and *R*(W-Co^{III})=5.19 Å, irrespective of the three phases. The local structure of the relaxed excited state was found to be identical with that of the high-temperature (300 K) phase. The phase transformation is concluded to be caused by the charge transfer and the spin flipping from the -W^{IV}(*S*=0)-CN-Co^{III} (*S*=0)- configuration to -W^{V}(*S*=1/2)-CN-Co^{II} (*S*=3/2)-.

Keywords: prussian blue, ferrimagnet, spin transition, relaxed excited state

1. Introduction

Prussian blue analogs have recently attracted great interest because of their various characteristics as molecular and metal-complex magnets. Sato *et al*. (1996) discovered the induction of a magnetic phase transition in FeCo cyanides by optical stimuli; although the Na and K salts of FeCo cyanides are paramagnetic down to 2 K, they become a ferrimagnet upon visible-light irradiation. Up to ~100 K, the ferrimagnetic behavior is preserved. Moreover, upon irradiation of near-infrared light, the phases turn back to the paramagnetic ones. Previously we performed Fe and Co K-edge XAFS analyses of these FeCo cyanide systems and determined local structure of low-temperature (LT) and high-temperature (HT) phases and of the relaxed photo-excited state (Yokoyama *et al*., 1998; Yokoyama *et al*., 1999).

Very recently, Hashimoto *et al*. (2000) synthesized another type of materials that show photo-induced magnetization. The material $Cs_{0.8}Co_{1.3}[W(CN)_8](3\text{-cyanopyridine})_{1.9}\cdot 2.1H_2O$ consists of $W(CN)_8$ complex anions which are linked with each other via Co ions. This shows the first-order transition at $T_{c}\downarrow$=205 K and $T_{c}\uparrow$=150 K with a large histeresis. Upon visible-light irradiation at low temperature, however, the HT phase is obtained as a metastable state, which exhibits ferrimagnetism. Since the sample is prepared only as a fine crystalline powder similar to other prussian-blue analogues, structure analysis by means of XAFS spectroscopy is essentially important to understand the mechanism of the photo-induced magnetization.

In this Proceeding, the results of XAFS analysis for the CoW cyanide are presented. The local structure of the LT and HT phases were determined. Moreover, we observed x-ray induced phase transformation at low temperature. Thus the results of the relaxed x-ray excited phase are also given instead of the visible-light excited state.

2. Experimental

The preparation method of the CoW cyanide will be reported elsewhere (Hashimoto *et al*., 2000). Co *K*- and W $L_{III,II}$-edge XAFS spectra were taken in the conventional transmission mode at the Beamline 12C of the Photon Factory (operation energy of 2.5 GeV and stored current of 400-200 mA). Si(111) double crystals were employed as a monochromator. Higher-order harmonics were eliminated by using the Rh-coated focusing mirror and by detuning of the double crystal. The intensities of the incident and transmitted x rays were recorded using ionization chambers filled with N_2.

The sample was dispersed on a scotch tape and several sheets of the tapes were piled up to obtain sufficient edge jumps of ~0.3 for both edges. The spectra of the HT and LT phases were recorded at 300 and 150 K, respectively. At 150 K, even if the excitation to the high-temperature phase by x-ray irradiation occurs during the measurements, the deexcitation rate back to the LT phase was found to be fast enough to record the spectra. For the relaxed x-ray excited phase, the sample was irradiated by x rays (~7800 eV) at 30 K for around two hours. At 30 K, the deexcitation rate was slow enough to accumulate the relaxed state.

3. Analysis and results

Figure 1 shows Co *K*-edge XANES spectra of the CoW cyanide at 300 and 150 K, together with the sample irradiated by x rays at 30 K. The spectrum at 300 K is clearly different from the one at 150 K; the intense resonance at ~7719 eV for the 300-K spectrum shifts to ~7723 eV for the 150-K one. The two-hour x-ray irradiated one closely resembles the 300-K one. Such spectral changes are similar to the previous CoFe case where the Co ions turns from the high-spin (HS) divalent state at 300 K to the low-spin (LS) trivalent one at low temperature. We can here present the same conclusion. The XANES spectra allow us to estimate the Co(II)/Co(III) composition ratios quantitatively through the factor analysis (Fernández-García *et al*., 1995; Yokoyama *et al*., 1998) using lots of data sets recorded during the x-ray irradiation. The results of the Co(II) ratios are 81.9% at 300 K, 32.7% at 150 K, and 67.0% for the x-ray irradiation.

The EXAFS analysis was carried out also in a similar manner to our previous papers (Yokoyama *et al*., 1998; Yokoyama *et al*., 1999). The EXAFS oscillation functions $k^3\chi(k)$ were obtained by means of standard analysis procedures using the analysis code EXAFSH (Yokoyama *et al*., 1993): pre-edge baseline subtraction, post-edge background estimation using cubic spline functions and the normalization with the atomic absorption coefficients. Figure 2 shows the W L_{III}-edge EXAFS functions $k^3\chi(k)$ and their Fourier transforms for 300 and 150 K and the x-ray-irradiated sample, together with the standard material of $Cs_3W(CN)_8$. In the Fourier transforms of the W L_{III}-edge EXAFS, one can find three dominant contributions at ~1.8, ~3.0 and ~5 Å, which are attributed to the W-C, W-N and W-Co shells, respectively. Because of a (nearly) linear configuration of the -W-C-N-Co- chain, the W-N and W-Co shells are noticeably enhanced due to the multiple-scattering focusing effect. The features of the W-C and W-N shells among the four spectra do not differ so much from each other, this indicating little

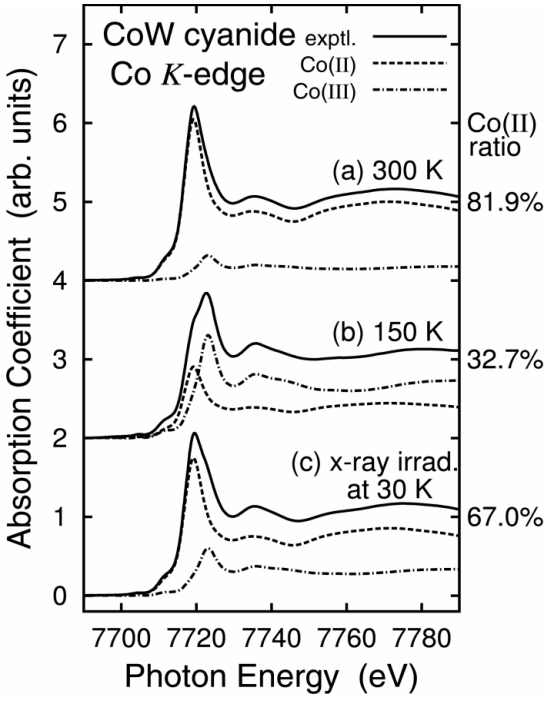

Figure 1
Co *K*-edge XANES spectra of the CoW cyanide (a) at 300 K, (b) at 150 K, and (c) after x-ray irradiation at 30 K for two hours. The results of the factor analysis are also given. The Co(II) composition ratio is given numerically, and the estimated pure Co(II) and Co(III) spectra are plotted as dashed and dot-dashed lines, respectively, where the edge jumps correspond to the composition ratios.

structure change of the $W(CN)_8$ unit irrespective of the charge difference. On the other hand, the W-Co shell exhibits clear differences. This indicates significant structural changes around Co.

In order to obtain the interatomic distance of each shell, the curve-fitting analysis was performed in *k* space including the error analysis. The statistical error ε^{st} for the transmission mode using ionization chambers was estimated by using the formula

$$(\varepsilon^{st})^2 = \frac{E(\mathrm{eV})}{1.92\times10^{15}}\left[\frac{10^{n_1} f_1^2}{I_0} + \frac{10^{n_2} f_2^2}{I}\frac{\mu}{(\mu-\mu_{\mathrm{VIC}})^2}\right] \quad (1)$$

where I_0 and I are respectively the intensity counts of incident and transmitted x rays (the amplifier gains n_1 and n_2), E the x-ray energy, μ the observed total absorption coefficient, and μ_{VIC} the extrapolated pre-edge baseline absorption. f_1 and f_2 are the user defining constants to scale the error bar. In the present analysis, the systematic errors ε^{sy} are also added. This is assumed to be

$$(\varepsilon^{sy})^2 = \frac{f_3^2\mu}{(\mu-\mu_{\mathrm{VIC}})^2}\frac{1}{k^{2n}}, \quad (2)$$

where n is the k weight (n=2 was assumed) and f_3 the user defining scaling parameter. The total error ε is given as

$$\varepsilon^2 = (\varepsilon^{st})^2 + (\varepsilon^{sy})^2 . \quad (3)$$

The optimized parameters are obtained by minimizing a standard residual factor R_f defined as

$$R_f = \sqrt{\sum_{i=1}^{N_{data}}(\chi_{obs}(k_i)-\chi_{calc}(k_i))^2 \Big/ \sum_{i=1}^{N_{data}}(\chi_{obs}(k_i))^2} , \quad (4)$$

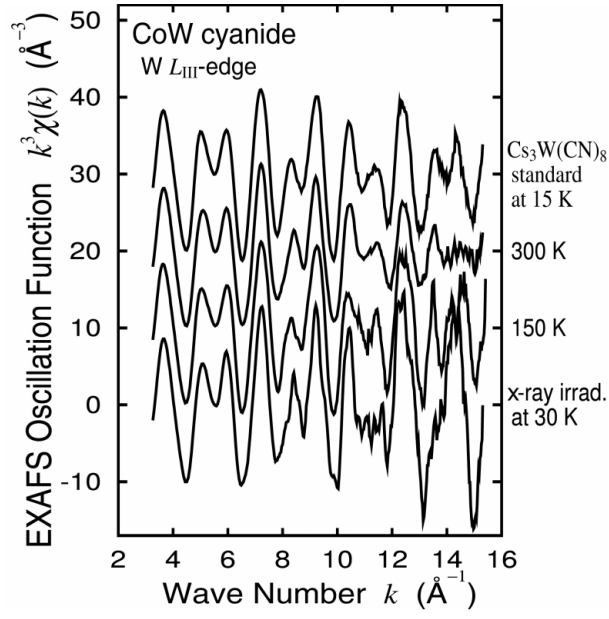

Figure 2
W L_{III}-edge EXAFS oscillation functions $k^3\chi(k)$ of the CoW cyanide: (b) 300 K, (c) at 150 K, and (d) after x-ray irradiation at 30 K. $k^3\chi(k)$ of the standard sample $Cs_3W(CN)_8$ is also shown in (a).

while the error estimation is done using the criteria formula

$$\chi_\mu^2 = \frac{N_{para}}{N_{data}(N_{ind}-N_{para})}\sum_{i=1}^{N_{data}}\left(\frac{\chi_{obs}(k_i)-\chi_{calc}(k_i)}{\varepsilon(k_i)}\right)^2 , \quad (5)$$

where N_{data}, N_{para} and N_{ind} are the numbers of data points, fitting parameters and independent data points, respectively. The error bar of each fitting variable is determined so that $\chi_\mu^2-\chi_\mu^2(\mathrm{opt})\cong1$.

For the backscattering amplitudes and phase shifts, theoretical EXAFS spectra were calculated using FEFF8 (Ankudinov *et al*., 1998) for a $W(CN)_8Co_8$ cubic cluster. For the W-C (ΔR_{FT}=1.3-2.1 Å) and W-N (ΔR_{FT}=2.3-3.4 Å) shells, single-shell fitting was performed in the *k* range of 4-15 Å^{-1}. For the W-Co (ΔR_{FT}=4.5-5.3 Å) shell two-shell fitting is required because of the presence of inequivalent W-Co(II) and W-Co(III) shells. The coordination numbers N and the edge-energy shift ΔE_0 were fixed, while the distance R and the Debye-Waller factor C_2 were optimized for the fitting k range of 4-15 Å^{-1}. Higher-order cumulants were neglected. For the W-C and W-N shells, the intrinsic loss factor S_0^2 and ΔE_0 were set to the values obtained in the analysis of the standard $Cs_3W(CN)_8$ (S_0^2=1.0±0.1). For the W-Co shell, S_0^2 and ΔE_0 were set to those for the W-N results. The curve-fitting results of the W L_{III}-edge EXAFS are tabulated in Table 1.

The W-C and W-N distances are found to be unchanged amongst all the phases: R(W-C)=2.16 Å and R(W-N)=3.32 Å. These values are also identical to those of the standard $Cs_3W(CN)_8$. The W-Co distances were determined as R(W-Co^{II})=5.37 Å and R(W-Co^{III})=5.19 Å, which are also independent of the phase. Note that although the W-Co^{III} distance at 300 K deviates significantly from the one at 150 K, this originates from a large error bar due to a small coordination number. It can be remarked that the present error analysis worked well. Although details of the Co *K*-edge EXAFS analysis is reported elsewhere, the first-nearest neighbor Co^{II}-N,O and Co^{III}-N,O distances (O is derived from the coordination of H_2O

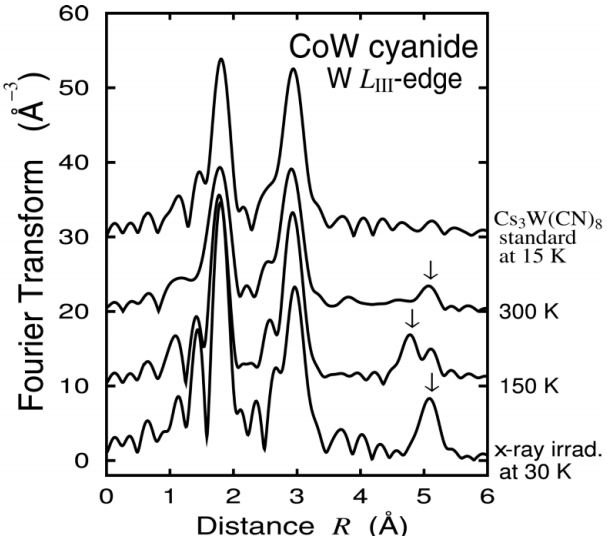

Figure 3
Fourier transforms of Fig. 2.

Table 1
The results of the W L_{III}-edge EXAFS analysis of the CoW cyanide. The coordination number N was fixed.

Sample	Shell	N	R (Å)	C_2 (10^{-2} Å^2)
$Cs_3W(CN)_8$	W-C	(8)	2.163(7)	0.21(7)
30 K	W-N	(8)	3.319(9)	0.34(9)
CoW cyanide	W-C	(8)	2.163(7)	0.21(7)
150 K	W-N	(8)	3.315(14)	0.46(8)
	W-Co^{II}	(0.981)	5.37(5)	0.21(42)
	W-Co^{III}	(2.019)	5.19(4)	0.44(39)
CoW cyanide	W-C	(8)	2.161(13)	0.34(14)
300 K	W-N	(8)	3.310(10)	0.45(10)
	W-Co^{II}	(2.457)	5.37(4)	0.90(42)
	W-Co^{III}	(0.543)	5.01(33)	1.23(339)
CoW cyanide	W-C	(8)	2.160(12)	0.01(11)
X ray	W-N	(8)	3.315(11)	0.34(11)
irradiation	W-Co^{II}	(2.000)	5.39(3)	0.33(20)
	W-Co^{III}	(1.000)	5.27(13)	0.71(120)

molecules) were tentatively determined as 2.14 and 1.95 Å, respectively. When the W-C-N-Co chain is assumed to be linear, the Co-N distances can be estimated to be 2.06 and 1.88 Å for Co(II) and Co(III), respectively, which are close to those obtained for the Co K-edge EXAFS analysis. Small differences might originate from a small off-linear configuration and the analytical errors.

4. Discussion

The present XAFS analysis confirms that the phase transition of the CoW cyanide at ~200 K is ascribed to the charge transfer and spin flipping origins from the -Co^{II}(S=3/2)-NC- W^{V}(S=1/2)- configuration (HT phase) to the -Co^{III}(S=0)-NC- W^{IV}(S=0)- one (LT). The Co(II) ions at the HT phase should be of high spin, while the Co(III) ions at the LT phase are of low spin. The Co^{II}(HS) ionic radius was found to be noticeably larger (by ~0.2 Å) than the Co^{III}(LS) one. Although the charge transfer indicates the change of the W valency as well, the W^{V}-C and W^{IV}-C distances were found to be almost equivalent to each other. This is also the case with the previous CoFe cyanide system where Fe^{II}(LS)-C and Fe^{III}(LS)-C distances are almost equal to each other.

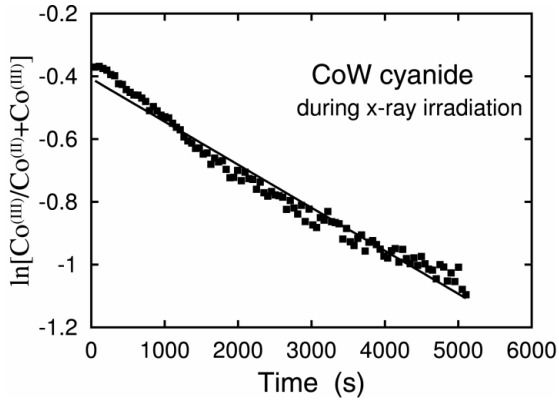

Figure 4
Time dependence of the Co(III) logarithmic ratio in the CoW cyanide during x-ray irradiation. The Co(III) ratio was determined by the continuous XANES measurements and the factor analysis. Experimental data are given as a filled square and a solid line is the least-squared linear function, which indicates a simple first-order kinetics.

The observation of x-ray induced excitation to the HT phase is interesting. Core-hole creation and subsequent Auger deexcitation consequently yields the charge transfer and high-spin phase. The local structure of the relaxed x-ray excited state was found to be essentially the same as the HT one. This is also found in the FeCo cyanide where the relaxed excited phase is obtainable with visible-light irradiation (not x rays).

Finally, let us briefly discuss the phase transformation with x-ray irradiation at 30 K. Figure 4 shows time dependence of the Co(III) ratio during the x-ray irradiation at 30 K. The logarithmic ratio of Co(III) decreases almost linearly with time, this indicating a simple first-order kinetics. Although the transition at ~200 K is clearly the first order, the formation of the relaxed excited state by x-ray irradiation does not seem abrupt but a continuous phase transformation should take place.

The present work has been performed under the approval of Photon Factory Program Advisory Committee (PF-PAC No. 2000G071).

References

Ankudinov, A. L., Ravel, B., Rehr, J. J. & Conradson, S. D. (1998). Phys. Rev. B58, 7565-7576.
Fernández-García, M., Márquez Alvarez, C. & Haller, G. L. (1995). *J. Phys. Chem.* **99**, 12565-12569.
Hashimoto, K., Ohkoshi, S. *et al*. (2000). *To be published.*
Sato, O., Iyoda, T., Fujishima, A. & Hashimoto, K. (1996).. *Science* **272**, 704-705.
Yokoyama, T., Hamamatsu, H. & Ohta, T. (1993). EXAFSH version 2.1, The University of Tokyo.
Yokoyama, T., Ohta, T., Sato, O. & Hashimoto, K. (1998). *Phys. Rev.* **B58**, 8257-8266.
Yokoyama, T., Kiguchi, M., Ohta, T., Sato, O., Einaga, Y. & Hashimoto, K. (1999). *Phys. Rev.* **B60**, 9340-9346.

Received 31 July 2000 • Accepted 8 November 2000